

# **DNAPLplume: Spreadsheet Model for Dissolved Plume Attenuation with DNAPL Source Remediation, Aqueous Decay and Volatilization – Model Calibration and First-Order Error Analysis**

Jack Parker, April 2009

## **1. Introduction**

Dense nonaqueous phase liquids (DNAPLs) pose a difficult groundwater remediation challenge due to the impracticability of complete DNAPL source removal and to the long-term persistence of contaminant fluxes when even small DNAPL amounts remain (e.g., Soga et al., 2004). The effectiveness of natural attenuation and the feasibility of engineered remediation strategies are contingent on a number of physical and biological processes that control net source zone mass flux and attenuation within the dissolved phase plume.

A number of recent studies have focused on relationships between contaminant mass flux from DNAPL sources and the amount and distribution of DNAPL remaining in the source. Sale and McWhorter (2000) presented a semi-analytical model for dissolution rates in sources with spatially distributed DNAPL within uniform velocity fields. Their results indicated that while near-equilibrium mass transfer may occur at the local-scale, field-scale mass transfer is primarily controlled by advective-dispersive transport and the geometry of the DNAPL zones. The authors concluded that field-scale dissolution rates will diminish little over time as a function of source mass depletion. Rao and Jawitz (2003) noted that this conclusion is conditioned on assumptions of uniform flow and spatially distributed DNAPL subzones that are uniform in terms of their size, geometry and mass. When these assumptions are not met, greater reductions in contaminant fluxes over time may occur as DNAPL is more quickly depleted in regions with higher velocities and/or smaller initial masses.

Parker and Park (2004) and Park and Parker (2005) presented a field-scale mass transfer function (Parker-Park model) for DNAPL dissolution kinetics and demonstrated its ability to quantify effects of DNAPL mass depletion over time, groundwater velocity within the source zone, and variations in source zone “architecture” based on high resolution numerical simulation results. The foregoing or similar mass flux versus mass depletion relationships have been utilized by a number of authors (Rao et al. 2001, Zhu and Sykes 2004, Jawitz et al. 2005, Falta et al. 2005ab, Christ et al. 2006, Fure et al. 2006, Basu et al. 2007, Saenton and Illangasekare 2007).

While many studies have addressed the biotransformation of chlorinated solvents within dissolved phase plumes, relatively few studies have considered effects of biodecay within DNAPL source areas. Semprini et al. (1992), Mravik et al. (2003) and Ramsburg et al. (2004) have discussed various methods to enhance source zone biodecay. Mass losses due to

volatilization of organic chemicals from groundwater under natural or engineered conditions have also been studied (Jury et al., 1990; Conant et al., 1996; Auer et al., 1996; Parker, 2003). To our knowledge, no models have been presented that incorporate effects of both source zone biodecay and plume-wide volatilization losses on dissolved plume attenuation.

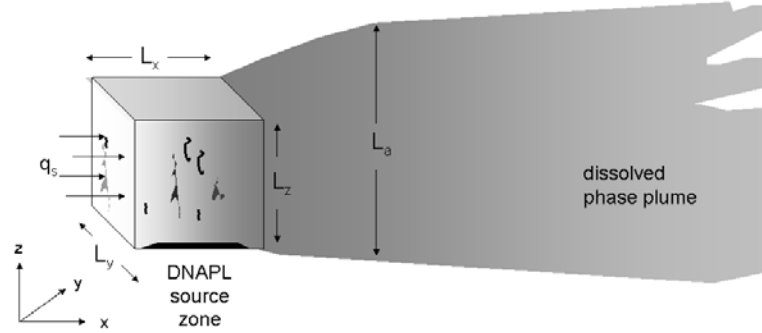


Figure 1. Source zone geometry.

## 2. Model Description

### 2.1 DNAPL Dissolution and Source Zone Biodecay

We consider a DNAPL source zone region of height  $L_z$  and width  $L_y$  with length  $L_x$  in the direction of groundwater flow in an aquifer of saturated thickness  $L_a$  (Figure 1). DNAPL, which is nonuniformly distributed within this region, undergoes mass transfer-limited dissolution to groundwater, and some of the dissolved mass biodegrades within the source zone before reaching the downgradient source zone boundary. Assuming linear field-scale mass transfer kinetics, first-order dissolved phase biodecay, and pseudo-steady-state advective transport, the areally-averaged source zone concentration distribution along the flow path may be approximated by

$$q_s \frac{dC}{dx} = \kappa_{eff} (C_{eq} - C) - \gamma_s \phi_s C \quad (1)$$

where  $q_s$  is the source zone darcy velocity [ $L T^{-1}$ ],  $C$  is aqueous phase concentration [ $M L^{-3}$ ],  $x$  is distance in the direction of flow [ $L$ ],  $C_{eq}$  is the equilibrium dissolved phase concentration [ $M L^{-3}$ ],

$\gamma_s$  is a source zone biodecay coefficient [ $T^{-1}$ ],  $\phi_s$  is source zone porosity [-], and  $\kappa_{eff}$  is an effective field-scale dissolution rate coefficient [ $T^{-1}$ ] that may be described (Parker and Park, 2004; Park and Parker, 2005) by

$$\kappa_{eff} = \kappa_o' q_s \left( \frac{M}{M_o} \right)^\beta \quad (2)$$

where  $\kappa_o'$  is a flow-normalized initial dissolution rate coefficient [ $L^{-1}$ ],  $M_o$  is initial DNAPL mass [M],  $M$  is the current DNAPL mass [M], and  $\beta$  is a mass depletion exponent [-]. Values of  $\beta$  greater than one reflect dissolution rates diminish more rapidly than relative mass reduction, while values less than one indicate disproportionately slower rate reductions. Studies by Park and Parker (2005) indicate  $\beta$  values greater than 1 for finger-dominated residual DNAPL and less than 1 for DNAPL pools and lenses, while Falta et al. (2005ab) suggest that sites with DNAPL located predominantly in low permeability zones exhibit  $\beta > 1$  while sites with DNAPL in higher permeability zones have  $\beta < 1$ . Integrating (1) along the source zone flow path gives

$$C(x') = \frac{C_{eq} \kappa_{eff}}{\kappa_{eff} + \gamma_s \phi_s} \left( 1 - \exp \left( \frac{-(\kappa_{eff} + \gamma_s \phi_s) x'}{q_s} \right) \right) \quad (3)$$

where  $C(x')$  is the mean concentration within the source perpendicular to the flow direction at a distance  $x'$  from the upgradient source boundary. The net contaminant flux from the source,  $J_{net}$  [ $M T^{-1}$ ], is

$$J_{net} = A_s q_s C_{out} \quad (4)$$

where  $A_s = L_y L_z$  is the gross source area perpendicular to the flow direction and  $C_{out} = C(x'=L_x)$ , which yields

$$J_{net} = \frac{q_s A_s C_{eq} \kappa_{eff}}{\kappa_{eff} + \gamma_s \phi_s} \left( 1 - \exp \left( \frac{-(\kappa_{eff} + \gamma_s \phi_s) L_x}{q_s} \right) \right). \quad (5)$$

A mass balance for the source may be written as

$$\begin{aligned} \frac{dM}{dt} &= -J_{tot} \\ &= -(J_{net} + J_{bio}) \end{aligned} \quad (6)$$

where  $J_{tot}$  is the contaminant dissolution rate [ $M T^{-1}$ ] and  $J_{bio}$  is the biodecay rate within the source zone [ $M T^{-1}$ ] given by

$$\begin{aligned}
J_{bio} &= C_{avg} V_s \phi_s \gamma_s \\
&= f C_{out} V_s \phi_s \gamma_s
\end{aligned} \tag{7}$$

in which  $V_s = L_x L_y L_z$  is the gross source zone volume [ $L^3$ ],  $C_{avg}$  is the average dissolved phase concentration within the source zone, and  $f = C_{avg}/C_{out}$  may be computed as

$$f = \frac{1}{LC_{out}} \int_0^{L_x} C(x') dx' . \tag{8}$$

Integration of (8) with (3) for  $C(x')$  gives

$$f = \frac{a - 1 + \exp(-a)}{a(1 - \exp(-a))} \tag{9}$$

where  $a = \kappa_{eff} L_x / q_s + \gamma_s \phi_s L_x / q_s$ . Eq. (9) indicates that  $f \rightarrow 0.5$  if

$\kappa_{eff} L_x / q_s \ll 1$  and  $\gamma_s \phi_s L_x / q_s \ll 1$  and  $f \rightarrow 1$  if  $\kappa_{eff} L_x / q_s \gg 1$  or  $\gamma_s \phi_s L_x / q_s \gg 1$ . If  $\kappa_o' L_x \ll 1$ , then

$\kappa_{eff} L_x / q_s \ll 1$  independent of source depletion and  $f$  will be controlled by the magnitude of

$\gamma_s \phi_s L_x / q_s$  over time as source depletion proceeds. Therefore, if  $\kappa_o' L_x < 1$ , we may disregard time-

dependence of  $f$  and employ  $a = \kappa_o' L_x + \gamma_s \phi_s L_x / q_s$  with little loss of accuracy. Note that if

$\kappa_{eff} L_x / q_s > 1$  with low biodecay, eq. (3) predicts the average source zone exit concentration will

approach equilibrium ( $C/C_{eq} > 0.63$ ). Since such average concentrations are rarely observed in

the field, we infer that the condition  $\kappa_{eff} L_x / q_s \ll 1$  is a valid approximation for most practical

purposes.

From (4) and (7), we observe that

$$F_{bio} \equiv \frac{J_{bio}}{J_{tot}} = \frac{f \gamma_s \phi_s L_x}{q_s + f \gamma_s \phi_s L_x} \tag{10}$$

which may be rearranged to compute  $\gamma_s$  from  $F_{bio}$ . The latter may be estimated from the ratio of total daughter product to primary contaminant species molar fluxes near the downgradient edge

of the source. Using  $F_{bio}$  we may express  $J_{net}$  in terms of  $J_{tot}$  as

$$J_{net} = (1 - F_{bio})J_{tot}. \quad (11)$$

If  $\kappa_o' L_x < 1$  (hence  $\kappa_{eff} L_x / q_s < 1$ ), then  $C(L_x) \ll C_{eq}$  in eq. (3) and the magnitude of source biodecay ( $\gamma_s$ ) will have little effect on the computed rate of source dissolution as represented by the first term on the RHS of (3). Under these conditions, the source dissolution rate can be computed using the model of Parker and Park (2004) given here in the simplified form

$$J_{tot}(t) = J_o \left( \frac{M(t)}{M_o} \right)^\beta \quad (12)$$

in which  $M(t)$  is the source mass at time  $t$ ,  $M_o$  is the source mass at the release date  $t = t_o$ , and  $J_o$  is the corresponding source dissolution rate [ $M T^{-1}$ ]. Substituting (12) into (11) yields

$$J_{net}(t) = (1 - F_{bio})J_o \left( \frac{M(t)}{M_o} \right)^\beta. \quad (13)$$

We caution that although field-scale concentration mass transfer gradients may not be significantly affected by source zone biodecay, *pore-scale* concentration gradients may be affected, which, in turn, impact *field-scale* mass transfer coefficients. For convenience in model calibration and to accommodate effects of remedial actions on dissolution kinetics, we recast (13) as

$$\begin{aligned} J_{net}(t) &= (1 - F_{bio\ 0})J_{cal} \left( \frac{M(t)}{M_{cal}} \right)^\beta & t_o < t \leq t_{rem} \\ &= (1 - F_{bio\ f})f_{mt}J_{cal} \left( \frac{M(t)}{M_{cal}} \right)^\beta & t > t_{rem} \end{aligned} \quad (14)$$

where  $J_{cal} = J_{tot}(t=t_{cal})$  and  $M_{cal} = M(t=t_{cal})$  in which  $t_{cal}$  denotes a reference time used for model calibration (e.g., when reliable field data becomes available),  $t_{rem}$  is the remediation date,  $F_{bio\ f}$  and  $F_{bio\ 0}$  are values of  $F_{bio\ f}$  before and after remediation, and  $f_{mt}$  is the ratio of the post- to pre-remediation mass transfer coefficients  $\kappa_{eff}$ . For example, Sorenson (2006) reported that enhanced source zone biodecay caused dissolution rate coefficients to increase by factors (i.e.,  $f_{mt}$ ) of 2 to 6 in laboratory studies and 3 to 8 in field studies. Also, Parker and Park (2004) have shown that field-scale dissolution rate coefficients vary in direct proportion to changes in source zone darcy flux. Thus, if remediation decreased source zone permeability by a factor of 2, for example,  $f_{mt}$  would be 0.5 in the absence of other effects.

Integration of (6) with (14) and (11) as described by Park and Parker (2005) gives source mass remaining versus time following the release date  $t_o$  subject to the stipulation that  $t_{cal} \leq t_{rem}$  as

$$\begin{aligned} &\text{for } t_0 < t \leq t_{rem} \\ M(t) &= \begin{cases} \left[ M_{cal}^{1-\beta} - (1-\beta)B(t-t_{cal}) \right]^{1/(1-\beta)} & \text{for } \beta \neq 1 \\ M_{cal} \exp(-B(t-t_{cal})) & \text{for } \beta = 1 \end{cases} \end{aligned} \quad (15)$$

$$\begin{aligned} &\text{for } t > t_{rem} \\ M(t) &= \begin{cases} \left[ M_{remf}^{1-\beta} - f_{mt}(1-\beta)B(t-t_{rem}) \right]^{1/(1-\beta)} & \text{for } \beta \neq 1 \\ M_{remf} \exp(-f_{mt}B(t-t_{rem})) & \text{for } \beta = 1 \end{cases} \end{aligned}$$

where  $B = J_{cal} / M_{cal}^\beta$ , and  $M_{remf}$  is the source mass following remediation computed by

$$\begin{aligned} M_{remf} &= M_{rem0} - \Delta M_{rem} \\ M_{rem0} &= \begin{cases} \left[ M_{cal}^{1-\beta} - (1-\beta)B(t_{rem}-t_{cal}) \right]^{1/(1-\beta)} & \text{for } \beta \neq 1 \\ M_{cal} \exp(-B(t_{rem}-t_{cal})) & \text{for } \beta = 1 \end{cases} \end{aligned} \quad (16)$$

where  $M_{rem0}$  is the source mass prior to remediation, and  $\Delta M_{rem}$  is the source mass eliminated by remediation initiated at  $t = t_{rem}$  and assumed to be effective immediately thereafter. The stipulation that  $t_{cal} \leq t_{rem}$  is made to avoid numerical problems that can arise if  $t_{rem}$  is inadvertently set to a date when the model parameters predict the source is depleted (e.g., during the process of model calibration). The requirement does not limit the model applicability or the use of post-remediation data for calibration.

The net source flux reduction caused by remediation may be computed from (14) as

$$R_{Jrem} \equiv \frac{J_{netf}}{J_{net0}} = \frac{f_{mt}(1-F_{biof})}{(1-F_{bio0})} \left( \frac{M_{remf}}{M_{rem0}} \right)^\beta \quad (17)$$

where  $J_{net0}$  and  $J_{netf}$  denote the net source flux before and after remediation.

## 2.2 Volatilization from Groundwater

Volatilization from groundwater is modeled following the approach of Parker (2003), which takes into consideration dissolved phase vertical dispersion within the aquifer, vadose zone vapor diffusion and dispersion, vapor phase advection driven by cyclic barometric pressure or water table fluctuations, and aqueous phase advection in the unsaturated zone. Resulting volatilization losses from groundwater follow the first-order kinetic expression

$$s_{vol} = \lambda_{vol} \phi_a C_z \quad (18)$$

where  $s_{vol}$  is the rate of mass loss per aquifer volume due to volatilization [ $\text{ML}^{-3}\text{T}^{-1}$ ],  $\lambda_{vol}$  is a volatilization coefficient [ $\text{T}^{-1}$ ],  $\phi_a$  is aquifer porosity [-], and  $C_z$  is the dissolved phase concentration [ $\text{ML}^{-3}$ ] at depth  $z$  below the water table (we disregard capillary fringe thickness here for simplicity). The volatilization coefficient may be formulated as

$$\begin{aligned} \lambda_{vol} &= \frac{q_u \kappa_{sat}}{\phi_a L_a \left( \exp \left( \frac{q_u L_u}{D_{eff} H} \right) - 1 \right)} & \text{for } q_u \neq 0 \\ \lambda_{vol} &= \frac{D_{eff} H \kappa_{sat}}{\phi_a L_a L_u} & \text{for } q_u = 0 \end{aligned} \quad (19)$$

where  $q_u$  is the unsaturated zone darcy velocity (+ downwards) [ $\text{L T}^{-1}$ ],  $L_u$  is the unsaturated zone thickness (distance from ground surface to water table) [ $\text{L}$ ],  $L_a$  is the saturated zone thickness over which volatilization losses are averaged [ $\text{L}$ ],  $H$  is a dimensionless Henry's coefficient for the chemical of concern [-],  $D_{eff}$  is an effective diffusion coefficient for vapor transport in the unsaturated zone [ $\text{L}^2\text{T}^{-1}$ ], and  $\kappa_{sat}$  is a nonequilibrium factor for vertical mass transfer within the aquifer [-]. Note that  $L_a$  may represent the entire aquifer thickness for a vertically-integrated model or the saturated thickness of the upper model layer for a vertically-discretized model. The effective vapor phase diffusion coefficient is defined by

$$D_{eff} = D_{diff} + D_{disp} \quad (20)$$

where  $D_{diff}$  is the porous media molecular diffusion coefficient [ $\text{L}^2\text{T}^{-1}$ ] estimated by the Millington-Quirk model as

$$D_{diff} = \phi_v^{10/3} \phi_u^{-2} D_v \quad (21)$$

where  $\phi_v$  and  $\phi_u$  are the air-filled and total porosities, respectively, in the unsaturated zone [-], and  $D_v$  is the molecular diffusion coefficient in free air [ $\text{L}^2\text{T}^{-1}$ ]. Assuming a linear increase in vapor dispersivity with travel distance, vapor phase dispersion is described by

$$D_{disp} = a\varepsilon L_u \quad (22)$$

where  $a$  is the effective vapor phase velocity [ $L T^{-1}$ ], and  $\varepsilon$  is the ratio of vertical dispersivity to travel distance [-] for vapor transport. For cyclic atmospheric pressure fluctuations,  $a$  may be approximated by

$$a = \frac{\phi_v \Delta P x_{bp}}{P_o t_{bp}} \quad (23)$$

where  $\Delta P$  is the pressure fluctuation range [ $F L^{-2}$ ],  $P_o$  is mean atmospheric pressure [ $F L^{-2}$ ],  $t_{bp}$  is the period of pressure fluctuations [T], and  $x_{bp}$  is the depth [L] of pressure fluctuation propagation estimated as

$$x_{bp} = \min \left( L_u, \frac{k_a \Delta P t_{bp}}{2 \phi_v \mu_a} \right) \quad (24)$$

in which  $k_a$  is the unsaturated zone vertical air permeability [ $L^2$ ], and  $\mu_a$  is the dynamic air viscosity [ $ML^{-1}T^{-1}$ ]. For cases in which water table fluctuations have a large magnitude and/or frequency (e.g., tidal zones), vapor dispersion may be described alternatively by

$$a = \frac{2 \phi_v \Delta x_{wt}}{t_{wt}} \quad (25)$$

in which  $\Delta x_{wt}$  is the magnitude of water table fluctuations [L], and  $t_{wt}$  is the period [T]. The mass transfer efficiency in (19) is defined by

$$\begin{aligned} \kappa_{sat} &= \frac{1}{1 + I_{sat} / I_{soil}} \\ I_{sat} &= \frac{HL_a / 2}{D_{wo} \phi_a^{4/3} + A_v q_a} \\ I_{soil} &= \frac{H}{q_u} \left( \exp \left( \frac{q_u L_u}{D_{eff} H} \right) - 1 \right) \quad \text{for } q_u \neq 0 \\ I_{soil} &= \frac{L_u}{D_{eff}} \quad \text{for } q_u = 0 \end{aligned} \quad (26)$$

where  $I_{sat}$  and  $I_{soil}$  are impedances to transport in the saturated and unsaturated zones, respectively,  $D_{wo}$  is the free water molecular diffusion coefficient [ $L T^{-2}$ ],  $A_v$  is aquifer vertical dispersivity [L], and it has been assumed that the vertically-averaged dissolved concentration in (18) corresponds to the concentration at a depth  $L_a/2$  below the water table.



### 2.3 Dissolved Phase Transport

We consider advective-dispersive dissolved phase transport in a steady-state planar velocity field downgradient of the source zone. If locations of interest are sufficiently far downgradient of the source that vertical mixing may be assumed, a 2-D transport equation may be employed as

$$R \frac{\partial C}{\partial t} = v \frac{\partial C}{\partial x} - A_L v \frac{\partial^2 C}{\partial x^2} - A_T v \frac{\partial^2 C}{\partial y^2} - \lambda_T(x)C + \frac{s(t)}{\phi_a} \quad (27)$$

where  $C$  is dissolved phase concentration [ $\text{ML}^{-3}$ ],  $R$  is a retardation factor [-],  $v$  is aquifer pore velocity [ $\text{LT}^{-1}$ ] (darcy velocity divided by aquifer porosity),  $A_L$  is longitudinal dispersivity [L],  $A_T$  is transverse dispersivity [L],  $s(t)$  is the time-dependent source net flux per unit aquifer volume [ $\text{MT}^{-1}\text{L}^{-3}$ ],  $x$  is distance from the downgradient plane of the source [L],  $y$  is distance from the center of the source in the transverse direction [L],  $t$  is time [T], and  $\lambda_T(x) = \lambda_{vol} + \lambda_{bio}$  where  $\lambda_{vol}$  is the groundwater volatilization coefficient [ $\text{T}^{-1}$ ] and  $\lambda_{bio}$  is a first-order biodecay coefficient for the dissolved plume [ $\text{T}^{-1}$ ], both treated as functions of longitudinal position. Specifically, we consider multiple “zones” along the axis of the plume reflecting variations in geochemical conditions (e.g., redox, DOC) that affect microbial activity or reflecting differences in conditions that affect volatilization. We also consider changes in coefficients that may occur following remedial action.

Falta et al. (2005b) presented a solution for dissolved transport with a depleting DNAPL source with constant coefficients based on Dominico (1987). Here we employ a time-convolution method for a time-dependent flux applied uniformly over the thickness of the aquifer at  $x=0$  between  $-L_y/2 < y < L_y/2$  for a contaminant-free initial condition to obtain a 2-D solution for the first aquifer “zone” located within the region  $0 < x \leq L_I$  as

$$C_1(x, y, t) = \int_0^t \frac{J_{net1}(t-\tau)}{4L_z L_y \phi_a (\pi R A_L v)^{1/2}} \exp\left(-\frac{\lambda_{T1}(\tau)\tau}{R} - \frac{(Rx - v\tau)^2}{4R A_L v \tau}\right) \times \left[ \text{erfc}\left(-\frac{y + L_y/2}{2(A_T v \tau / R)^{1/2}}\right) - \text{erfc}\left(-\frac{y - L_y/2}{2(A_T v \tau / R)^{1/2}}\right) \right] \frac{d\tau}{\tau^{1/2}} \quad (28)$$

where  $\tau$  is a dummy variable,  $J_{net1}(t-\tau)$  is the net source mass flux ( $\text{MT}^{-1}$ ) at time  $t-\tau$  computed from (14) through (16), and  $\lambda_{T1}(\tau)$  is the zone 1 decay coefficient ( $\lambda_{vol1} + \lambda_{bio1}$ ) that is taken as the pre-remediation value ( $\lambda_{T10}$ ) at  $\tau \leq t_{rem}$  and as the post-remediation ( $\lambda_{T1f}$ ) value thereafter. To obtain the solution in the second zone at  $x > L_I$ , (28) is employed using the zone 2 decay coefficient ( $\lambda_{T20}$  and  $\lambda_{T2f}$  before and after remediation, respectively) in lieu of  $\lambda_{T1}$  and with a modified source function  $J_{net2}$  adjusted to correct for the difference in mass flux at  $x = L_I$  using

$\lambda_{T1}$  versus  $\lambda_{T2}$  as follows

$$\begin{aligned} C_2(x, y, t) &= C_1(x, y, t; \lambda_{T2}, J_{net2}(\tau)) \\ J_{net2}(\tau) &= J(\tau; F_2 J_{cal1}, F_2 M_{cal1}) \\ F_2 &= \frac{C_1(L_1, 0, t; \lambda_{T1}, J_{net1}(\tau))}{C_1(L_1, 0, t; \lambda_{T2}, J_{net1}(\tau))} \end{aligned} \quad (29)$$

where  $C_1(x, y, t; \lambda, J(\tau))$  denotes the solution to (28) for specified values for  $x$ ,  $y$  and  $t$  with the specified decay coefficient  $\lambda$  and net source flux function versus time  $J(\tau)$  with other parameters identical for both zones;  $J_{net2}(\tau)$  is a fictitious source function that adjusts for mass

lost in zone 1;  $J(\tau; J_{cal}, M_{cal})$  represents the solution to (14) - (16) with specified values of  $J_{cal}$  and  $M_{cal}$ ;  $J_{cal1}$  and  $M_{cal1}$  represent values of  $J_{cal}$  and  $M_{cal}$  that describe the actual source behavior;  $J_{net1}(\tau) = J(\tau; J_{cal1}, M_{cal1})$  is the actual net source function; and  $F_2$  is a flux adjustment factor. Note that (29) constrains the solution to conserve mass and maintain continuity of concentrations in time and space. Additional zones may be considered using the preceding zone solution by incrementing subscripts in (29). Spatial variations in other parameters can be treated in a similar manner subject to the constraint that the ratio of darcy velocity to aquifer thickness must remain constant to maintain a mass balance with the planar flow field.

In general, the average groundwater flow direction over the history of the plume is not precisely known, resulting in uncertainty in the coordinate system orientation. Accordingly, we consider the translation from a working coordinate system ( $x'$ - $y'$ ) to a plume-oriented system ( $x$ - $y$ ) as

$$\begin{aligned} x &= x' \cos \alpha - y' \sin \alpha \\ y &= x' \sin \alpha + y' \cos \alpha \end{aligned} \quad (30)$$

where the coordinate origins are assumed to be identical (i.e., source location is known) and  $\alpha$  is a clockwise rotation angle.

### 3. Model Implementation

The DNAPL source and dissolved transport model described above was implemented in Excel/VBA as a function call. The format of the function is:

$$= \text{CNAPL}(J_{cal}, M_{cal}, \beta, L_y, L_z, t_0, t_{cal}, q_w, \phi, R, A_L, A_T, F_{bio0}, \lambda_1, L_{12}, \lambda_2, t_{rem}, \Delta M_{rem}, F_{mb}, F_{biof}, x, y, t, mode)$$

where  $x$  is distance (m) from the source downstream boundary in the direction of groundwater flow,  $y$  is lateral distance from the plume centerline,  $t$  is the date in decimal years,  $mode$  is a switch controlling function output, and all other parameters are described in Table 1.

The output modes are as follows:

If mode = 0 then CNAPL = Dissolved concentration at location (x,y) and time t ( $\mu\text{g/L}$ )

If mode = 1 then CNAPL =  $M_{\text{rem}0}$  (kg)

If mode = 2 then CNAPL =  $M_{\text{remf}}$  (kg)

If mode = 3 then CNAPL =  $R_{\text{jrem}}$  (-)

If mode = 4 then CNAPL = Source mass remaining at time t (kg)

If mode = 5 then CNAPL = Source flux from the source at time t (kg/d)

If mode = 6 then CNAPL = Flow-average exit concentration from source

Table 1. Summary of model parameters.

Description	Symbol	Units
Plume darcy velocity	$q_w$	m/d
Retardation factor	$R$	-
Longitudinal dispersivity	$A_L$	m
Transverse dispersivity	$A_T$	m
Zone 1 total decay coefficient	$\lambda_{T1}$	1/d
Zone 2 total decay coefficient	$\lambda_{T2}$	1/d
Ratio of source dissolution to source biodecay rates prior to remediation	$F_{bio\ 0}$	-
Source mass removed by source remediation	$\Delta M_{\text{rem}}$	kg
Ratio of mass transfer coefficient post- vs pre-remediation	$f_{mt}$	-
Date of DNAPL release	$t_o$	yr
Calibration date	$t_{\text{cal}}$	yr
Date of source remediation	$t_{\text{rem}}$	yr
Dissolution flux on calibration date	$J_{\text{cal}}$	kg/d
Source mass on calibration date	$M_{\text{cal}}$	kg
Source depletion exponent	$\beta$	-
Coordinate rotation	$\alpha$	degrees
Source width	$L_y$	m
Distance from downstream source boundary to zone 2	$L_{12}$	m
Aquifer thickness	$L_a$	m
Aquifer porosity	$\phi$	-
Ratio of source dissolution to source biodecay rates after remediation	$F_{bio\ f}$	-

Decay coefficients are lumped values representing biodecay within the aquifer and volatilization losses from the water table and ground surface, which may be computed from an associated worksheet external to the VBA code. Multiple DNAPL sources (which may be co-located in time and space or not) may be modeled by adding solutions for two or more function calls. Electron donor (ED) limited biodecay may similarly be modeling by superposition of solutions for contaminant transport and ED after adjusting the ED solution for the reaction stoichiometry (i.e., mass of TCE degraded per mass of ED).

#### 4. Model Calibration

Model calibration may be performed using a nonlinear regression method to minimize an objective function formulated as

$$O(\bar{p}) = \sum_{i=1}^{N_o} \frac{(Y_{obs\ i} - Y_i(\bar{p}))^2}{s_{oi}^2} + \sum_{j=1}^{N_p} \frac{(p_{prior\ j} - p_j)^2}{s_{pj}^2} \quad (31)$$

where  $\bar{p}$  is a vector of model parameters,  $Y_{obs\ i}$  is the  $i^{th}$  of  $N_o$  field observations with variance  $s_{oi}^2$  and corresponding model predictions  $Y_i(\bar{p})$ , and  $p_{prior\ j}$  is the prior estimate of the  $j^{th}$  of  $N_p$  model parameters with estimation variance  $s_{pj}^2$  and current regression parameter value  $p_j$ . The

first term in (31) reflects errors in model predictions and the second term is a “penalty function” that constrains parameters from moving too far from prior estimates considering the uncertainty in prior information (Sadeghipour and Yeh, 1984). We assume uncertainty in the depletion exponent, release date and coordinate rotation angle to be normally distributed. Predicted concentrations and all other model parameters are assumed to be log-normally distributed. Variables in (31) corresponding to the latter therefore represent natural log-transformed populations. For log-transformed variables, the inverse weighting factors therefore become the respective ln-variances, i.e.,  $s_{\ln x}^2$  rather than  $s_x^2$ . Minimization of (31) is performed using the Levenberg-Marquardt algorithm (Marquardt, 1963).

Logarithms of predicted and observed concentrations are included in the first term in the objective function. The  $s_{\ln o}^2$  for concentration data may be initially assumed to be 1 and subsequently refined using the root mean square  $\ln C$  regression error. The logarithm of remediation flux ratio ( $R_{Jrem}$ ) can be computed by eq (17) and incorporated in the first term of

the objective function. A prior estimate may be computed as the geometric mean ratio of dissolved concentrations after remediation versus those before remediation from near-source wells.

An estimate of the post-remediation source biodecay factor ( $F_{bio,f}$ ) may be obtained by measuring the ratio of TCE daughter products to TCE plus decay products in near-source wells. A prior estimate of the aquifer darcy velocity ( $q_w$ ) may be obtained from aquifer pump tests and natural gradient measurements. A prior estimate of the retardation factor for TCE ( $R$ ) may be determined from *in situ* push-pull tests, lab batch data or calculations from organic carbon data. Longitudinal and transverse dispersivities ( $A_L$  and  $A_T$ ) may be initially estimated from correlations with plume size (e.g., ~ 5 and 1 %, respectively). Estimates of aquifer biodecay coefficients may be obtained from push-pull or other field tests, and volatilization coefficients may be estimated from the volatilization model in conjunction with unsaturated zone data.

A prior estimate of the pre-remediation source decay ratio ( $F_{bio,0}$  – line 8) may be computed from measurements of TCE and daughter products in wells near the source and an estimate of source mass removal during source remedial action ( $\Delta M_{rem}$ ) may be obtained by analysis of source treatment process data, pre-/post-remediation soil boring data, or experience from similar sites and source treatment methods (e.g., thermal, chemical oxidation, etc.). The post- versus pre-remediation mass transfer ratio ( $f_{mt}$ ) is expected to be greater than 1 with various field and lab studies indicating values between 2-4 most likely.

The release date ( $t_o$ ) can often be bracketed based on site operational history and refined by calibration. The dissolution flux on the calibration date ( $J_{cal}$ ) may be estimated from measurements of primary contaminant and decay product concentrations near the source in conjunction with estimates of groundwater velocity and aquifer thickness, or via direct flux measurements (Annable et al., 2005). If the calibration date is selected to immediately precede remediation, the source mass on the calibration date ( $M_{cal}$ ) will correspond to the pre-remediation mass ( $M_{cal,0}$ ). Source mass is difficult to characterize accurately. Data from soil boring may be helpful, but even so, prior estimates will be uncertain and will need to be refined by calibration.

Site characterization data will often indicate whether DNAPL pools and/or lenses are likely at the site. The source depletion exponent ( $\beta$ ) will generally be between 0.5 and 1.0 for pools and between 1.0 and 1.5 for residual DNAPL. If both occur, then two source functions may be necessary for accurate calibration. Multi-level concentration or flux data will facilitate dual source calibration.

## 5. Uncertainty Analysis

We turn now to the quantification of model prediction uncertainty to assess the practical utility of the calibrated model. Following Hill (1998) and assuming log-normally distributed model predictions, we estimate total uncertainty for prediction  $k$  as

$$s_{T \ln C_k} = s_{R \ln C_k} + s_{P \ln C_k} \quad (32)$$

where  $s_{T \ln C_i}$  is the total  $\ln C$  uncertainty,  $s_{R \ln C_i}$  is the regression error, and  $s_{P \ln C_i}$  is the error due to parameter uncertainty. Note that the  $k^{th}$  prediction may correspond to a member of the calibration data set as well as to out-of-sample predictions.

The regression variance for prediction  $k$  with independent variables  $(x_k, y_k, t_k)$  is computed as

$$s_{R \ln C_k}^2 = MSE \left( 1 + \frac{1}{N_o} + \frac{(x_k - \bar{x})^2}{\sum_{i=1}^{N_o} (x_i - \bar{x})^2} + \frac{(y_k - \bar{y})^2}{\sum_{i=1}^{N_o} (y_i - \bar{y})^2} + \frac{(t_k - \bar{t})^2}{\sum_{i=1}^{N_o} (t_i - \bar{t})^2} \right) \quad (33)$$

where  $i = 1$  to  $N_o$  refers to observations used for calibration, overbars signify averages over the calibration data set, and MSE is the mean square error in concentrations used for calibration, computed as

$$MSE = \frac{\sum_{i=1}^{N_o} (\ln C_{obs\ i} - \ln C_{pred\ i})^2}{N_o - N_p} \quad (34)$$

where  $N_p$  is the number of calibrated parameters. Error due to parameter uncertainty is estimated using a first-order error propagation method (e.g., Unlu et al., 1995), which may be given in matrix notation as

$$\mathbf{s}_{P \ln C}^2 = \mathbf{J}^T \mathbf{Cov} \mathbf{J} \quad (35)$$

where the left-hand side is the vector of variances due to parameter uncertainty for all predictions of interest,  $\mathbf{J}$  is a Jacobian matrix, and  $\mathbf{Cov}$  is the parameter covariance matrix. Terms in the Jacobian are defined by

$$J_{ij} = \frac{\partial \ln C_i}{\partial P_j} \quad (36)$$

where  $P_j$  denotes uncertain parameter  $P$ , which as previously noted is either the actual parameter

value or its natural logarithm depending on the variable. The covariance matrix is estimated as

$$\mathbf{Cov} = \text{MSE}(\mathbf{J}^T \mathbf{J})^{-1}. \quad (37)$$

Confidence limits for predicted concentrations are estimated assuming log-normally distributed error as

$$CL_\alpha = \exp(\ln C_i \pm t_\alpha s_{T \ln C_i}) \quad (38)$$

where  $C_i$  is prediction  $i$  using best estimates of all model parameters, and  $t_\alpha$  is the  $t$ -statistic for probability  $1-\alpha$ .

## 6. References

- Annable, M. D., K. Hatfield, J. Cho, H. Klammler, B. L. Parker, J. A. Cherry, and P. S. C. Rao, 2005, Field-scale evaluation of the passive flux meter for simultaneous measurement of groundwater and contaminant fluxes, *Environ. Sci. Technol.*, 39 (18), 7194 -7201.
- Auer, L. H., N. D. Rosenberg, K. H. Birdsell and E. M. Whitney, 1996, The effects of barometric pumping on contaminant transport, *J. Contam. Hydrol.*, 24, 145-166.
- Basu, N.B, P.S.C. Rao, R.W. Falta, M. D. Annable, J. W. Jawitz, K. Hatfield, 2007, Temporal evolution of DNAPL source and contaminant flux distribution: Impacts of source mass depletion, *J Contam Hydrol.*, 95, 93-109.
- Christ, J. A., C. A. Ramsburg, K. D. Pennell, and L. M. Abriola (2006), Estimating mass discharge from dense nonaqueous phase liquid source zones using upscaled mass transfer coefficients: An evaluation using multiphase numerical simulations, *Water Resour. Res.*, 42, W11420, doi:10.1029/2006WR004886.
- Conant, B. H., R. W. Gillham and C. A. Mendoza, 1996, Vapor transport of trichloroethylene in the unsaturated zone: Field and numerical modeling investigations, *Water Resour. Res.*, 32, 9-22.
- Falta, R. W., P. S. Rao, and N. Basu, 2005a, Assessing the impacts of partial mass depletion in DNAPL source zones: I. Analytical modeling of source strength functions and plume response, *J. Contam. Hydrol.*, 78, 259-280.
- Falta, R. W., P. S. Rao, and N. Basu, 2005b, Assessing the impacts of partial mass depletion in DNAPL source zones: II. Coupling source strength functions to plume evolution, *J. Contam. Hydrol.*, 79, 45-66.

- Fure, A.D., J.W. Jawitz, and M.D. Annable. 2006. DNAPL source depletion: Linking architecture and flux response, *J. Contam. Hydrol.*, 85, 118-140
- Hill, M. C. 1998. Methods and guidelines for effective model calibration, U.S. Geological Survey, Water Resources Investigations Report 98-4005.
- Jawitz, J. W., A. D. Fure, G. G. Demmy, S. Berglund, and P. S. C. Rao, 2005, Groundwater contaminant flux reduction resulting from nonaqueous phase liquid mass reduction, *Water Resour. Res.*, 41, W10408, doi:10.1029/2004WR003825.
- Jury, W. A., D. Russo, G. Streile and H. El Abd, 1990, Evaluation of volatilization by organic chemicals residing below the soil surface, *Water Resources Research*, 26, 13-20.
- Mravik, S.C., R.K. Sillan, A.L. Wood and G.W. Sewell, 2003, Field evaluation of the solvent extraction residual biotreatment technology, *Environ. Sci. and Tech.*, 37 (21), 5040-5049.
- Parker, J. C., Physical processes affecting natural depletion of volatile chemicals in soil and groundwater, *Vadose Zone Journal*, 2, 222-230, 2003.
- Parker, J. C. and E. Park, 2004, Field-scale DNAPL dissolution kinetics in heterogeneous aquifers, *Water Resources Research*, vol 40, W05109, doi:10.1029/2003WR002807.
- Park, E. and J. C. Parker, 2005, Evaluation of an upscaled model for DNAPL dissolution kinetics in heterogeneous aquifers, *Adv. in Water Resources.*, 28, 1280-1291.
- Ramsburg, C. A., L. M. Abriola, K. D. Pennell, F. E. Loffler, M. Gamache, B. K. Amos, and E. A. Petrovskis, 2004, Stimulated microbial reductive dechlorination following surfactant treatment at the Bachman Road site, *Environ. Sci. and Tech.*, 38(22), 5902-5914.
- Rao, P. S. C., and J. W. Jawitz, 2003, Comment on “Steady-state mass transfer from single-component dense non-aqueous phase liquids in uniform flow fields” by T.C. Sale and D. B. McWhorter, *Water Resour. Res.*, 39, 1068, doi:10.1029/2001WR000599.
- Rao, P.S.C., J.W.Jawitz, C.G Enfield, R. Falta, M.D. Annable, A.L. Wood, 2001, Technology integration for contaminated site remediation” Cleanup goals and performance metrics, *Ground Water Quality*, Sheffield UK, p. 410-412.
- Saenton, S., and T. H. Illangasekare (2007), Upscaling of mass transfer rate coefficient for the numerical simulation of dense nonaqueous phase liquid dissolution in heterogeneous aquifers, *Water Resour. Res.*, 43, W02428, doi:10.1029/2005WR004274.
- Sale, T. C., and D. B. McWhorter, 2001, Steady state mass transfer from single-component dense nonaqueous phase liquids in uniform flow fields, *Water Resour. Res.*, 37(2), 393– 404.



- Sadeghipour, J., Yeh, W.W-G., 1984, Parameter identification of groundwater aquifer models: A generalized least squares approach, *Water Resources Research*, 20, 971-979.
- Semprini, L., G. D. Hopkins, P. V. Roberts, and P. L. McCarty, 1992, Pilot scale field studies of in-situ bioremediation of chlorinated solvents, *J. Hazardous Mat.*, 32(2-3), 145-162.
- Soga, K., J. W. E. Page, and T. H. Illangasekare, 2004, A review of NAPL source zone remediation efficiency and the mass flux approach, *J. Hazardous Mat.*, 110, 13-27.
- Sorenson, K. S., 2006, Recent progress in bioremediation of chlorinated solvent DNAPL source areas, *Partners in Environmental Technology Symposium and Workshop*, Nov 28-30, 2006, US Dept. of Defense – SERDP, C-46.
- Unlu, K., J. C. Parker, and P. K. Chong, A comparison of three uncertainty analysis methods to assess groundwater impacts from land-disposed waste, *Hydrogeology Journal*, 3(2), 1995.
- Zhu, J. and J.F. Sykes, 2004, Simple screening models of NAPL dissolution in the subsurface, *J. Contam. Hydrol.*, 72, 245-258.